SCHOMAKER, V. & TRUEBLOOD, K. N. (1968). *Acta Cryst.* B**24**, 63–76.
SCHULTZ, A. J., STUCKY, C. D., BLESSING, R. H. & COPPENS, P. (1976). *J. Am. Chem. Soc.* **98**, 3194–3201.
SHAANAN, B., SHMUELI, U. & RABINOVICH, O. (1976). *Acta Cryst.* B**32**, 2574–2580.
SPENCER, K., CAVA, M. P. & GARITO, A. F. (1976). *J. Chem. Soc. Chem. Commun.* pp. 966–967.
SPENCER, H. K., CAVA, M. P., YAMAGISHI, F. G. & GARITO, A. F. (1976). *J. Org. Chem.* **41**, 730–731.
WEGER, M. & FRIEDEL, J. (1977). *J. Phys. (Paris)*, **38**, 241–258.
WUDL, F., KAPLAN, M. L., HUFNAGEL, E. T. & SOUTHWICK, E. W. (1974). *J. Org. Chem.* **39**, 3608–3610.
WUDL, F., KRUGER, A. A., KAPLAN, M. L. & HUTTON, R. S. (1977). *J. Org. Chem.* **42**, 768–770.

Acta Cryst. (1978). B**34**, 2818–2825

The Crystal Structure and the Phase Transition of Ammonium 7,7,8,8-Tetracyanoquinodimethanide, NH_4–TCNQ

BY HAYAO KOBAYASHI

Department of Chemistry, Faculty of Science, Toho University, Funabashi, Chiba 274, *Japan*

(*Received* 18 *January* 1978; *accepted* 18 *April* 1978)

The crystals of ammonium 7,7,8,8-tetracyanoquinodimethanide (NH_4–TCNQ) show dimorphism. Purple crystals of NH_4–TCNQ–I were grown from a solution of tetrahydrofuran and methanol. The rotation and Weissenberg photographs showed that NH_4–TCNQ–I undergoes a monomer–dimer transition at 28 ± 5°C. The lattice spacing along the needle axis of the crystal which is parallel to columns of TCNQ molecules is 7·19 Å at 20°C and 3·61 Å at 38°C. Bluish-purple crystals of NH_4–TCNQ–II grown from an acetonitrile solution show sharp Bragg spots and diffuse streaks, which were explained on the basis of a disordered anti-phase domain structure. The average structure of NH_4–TCNQ–II deduced from the sharp spots is tetragonal with space group $P4/mbm$, $a = 12{\cdot}50 \pm 0{\cdot}02$ and $c = 3{\cdot}82 \pm 0{\cdot}04$ Å. TCNQ molecules are stacked face-to-face to form monadic columns along c. The mode of overlap of adjacent TCNQ molecules is of the ring–external-bond type. The intermolecular spacing is 3·31 Å. Evidence for a monomer–dimer transition of NH_4–TCNQ–II was obtained at about −58°C from resistivity measurements. On the basis of information obtained about the crystal structure and the magnetic susceptibilities, the monomer–dimer transitions of alkali-metal–TCNQ and NH_4–TCNQ can be considered to be spin–Peierls transitions.

Introduction

Recently, magnetic susceptibilities and phase transitions of one-dimensional compounds such as the radical anion salts of TCNQ and mixed-valence planar complexes of transition metals have aroused considerable interest (André, Bieber & Gautier, 1976; Keller, 1977). Some of these highly-conductive compounds undergo Peierls transitions, which indicates that the compounds are one-dimensional metal systems. The magnetic analog, the spin–Peierls transition of the Heisenberg antiferromagnetic linear-chain system, has also been observed (Bray, Hart, Interrante, Jacobs, Kasper, Watkins, Wee & Bonner, 1975). Both transitions are accompanied by distortion of the one-dimensional chains. The magnetic susceptibilities of alkali-metal–TCNQ compounds and related simple salts have been reported (Vegter, Kuindersma & Kommandeur, 1971; Vegter & Kommandeur, 1975; Kommandeur, 1975). Alkali-metal–TCNQ compounds, except Li–TCNQ, undergo phase transitions. Crystal structure analyses of the low- and high-temperature phases of Na–TCNQ and K–TCNQ (Konno & Saito, 1974, 1975; Konno, Ishii & Saito, 1977) indicate that the dimeric structures of the TCNQ columns revert to monomeric ones on passing through the transition temperatures. Besides alkali-metal–TCNQ, NH_4–TCNQ and Cu–TCNQ show similar phase transitions (Kommandeur, 1975).

It is reported in this paper that the crystals of NH_4–TCNQ are dimorphic, the purple NH_4–TCNQ crystals and bluish-purple NH_4–TCNQ crystals being denoted by NH_4–TCNQ–I and NH_4–TCNQ–II, respectively. In order to obtain a better knowledge of the physical properties of the simple salts of TCNQ, the crystal structure and the phase transition of NH_4–TCNQ were studied.

Experimental

Crystals of NH_4–TCNQ were prepared from NH_4I and TCNQ. Two kinds of crystals were obtained. When a

solution of tetrahydrofuran and methanol was used, the purple needles of NH_4–TCNQ–I were obtained. Oscillation and Weissenberg photographs of the NH_4–TCNQ–I crystals which were sealed in glass capillaries showed that the crystals were twinned; twinning planes were (110) and/or ($1\bar{1}0$). The patterns on the oscillation photographs changed on passing through 28 °C, indicative of a phase transition. The preliminary lattice constants were: low-temperature phase (orthorhombic), $a = 18{\cdot}19$ (1), $b = 17{\cdot}75$ (1), $c = 7{\cdot}19$ (1) Å, $Z = 8$ (20 °C); high-temperature phase (orthorhombic), $a = 18{\cdot}23$ (1), $b = 17{\cdot}80$ (1), $c = 3{\cdot}61$ (2) Å, $Z = 4$ (38 °C). A crystal structure analysis was not made because the crystals obtained were unsuitable.

The bluish-purple rods of NH_4–TCNQ–II were grown from an acetonitrile solution. The oscillation and Weissenberg photographs of NH_4–TCNQ–II show diffuse streaks parallel to a^* and to b^* (Fig. 1). Fairly sharp maxima are repeated regularly along the streaks. Disregarding the diffuse scattering, all the spots can be indexed with respect to the tetragonal unit cell with the dimensions listed in Table 1. The distributions of the diffuse streaks and the diffuse maxima are summarized in Table 2. Weissenberg intensity data were collected with Cu $K\alpha$ radiation. The intensities were estimated visually with a standard film strip and converted to $|F(hkl)|$ by applying the usual Lp and spot-shape corrections.

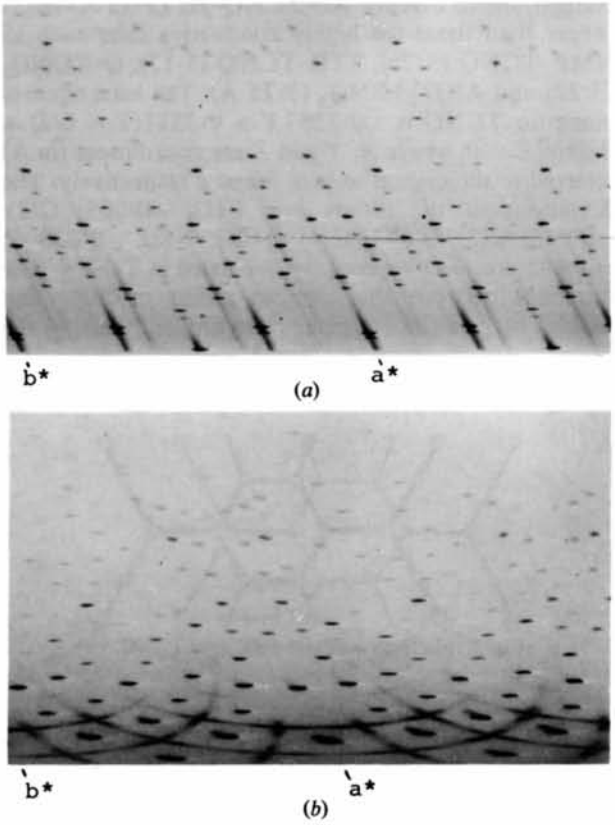

Fig. 1. Weissenberg photographs of NH_4–TCNQ–II. (*a*) *hk*0 layer: no extra reflections observable. (*b*) *hk*1 layer: diffuse maxima and streaks observable.

Determination of the average structure of NH_4–TCNQ–II

Diffuse streaks observed along a^* and b^* on the lth layer Weissenberg photographs around c ($l \neq 0$), indicate that domains with stacking disorder along a and b co-exist in the crystal. The diffuse maxima which were observed can be explained by the superposition of the superstructures with orthorhombic unit cells: (1) $a' = 2a$, $b' = 4a$, $c' = c$ and (2) $a' = 4a$, $b' = 2a$, $c' = c$.

The crystal structure analysis based on the sharp spots will give the 'average structure' of the disordered domain structures. The systematic absence of sharp spots ($h0l$, with $h = 2n + 1$) is characteristic of the space groups $P4/mbm$, $P4bm$ and $P\bar{4}b2$. Considering that the crystal structures of the simple salts of TCNQ resemble each other, the trial structure could be easily deduced from Patterson synthesis. The space group $P4/mbm$ was assumed and was confirmed by the convergence of the structure at a later stage of the refinement. The atomic parameters were refined by block-diagonal least-squares methods. However, those of C(1), C(4) and N(2), which are located near the mirror plane perpendicular to c, could not be refined. In a further refinement, the off-diagonal matrix elements related to z, U_{33}, U_{13} and U_{23} of these atoms were assumed to be zero. The hydrogen atoms of TCNQ were refined isotropically. The R value converged to 0·128 for 236 observed reflections. The atomic scattering factors used were those listed in *International*

Table 1. *Crystallographic data of the average structure of* NH_4–TCNQ–II

Formula: $NH_4.C_{12}H_4N_4$	FW 222·2
Tetragonal	
Space group: $P4/mbm$	
$a = 12{\cdot}50 \pm 0{\cdot}02$ Å	$D_m = 1{\cdot}25$ g cm^{-3}
$c = 3{\cdot}82 \pm 0{\cdot}04$	$D_x = 1{\cdot}24$
$U = 597{\cdot}2$ Å^3	$Z = 2$

Table 2. *Summary of reflections*

The Bragg indices refer to the unit cell listed in Table 1. The diffraction vector is $\lambda(pa^* + qb^* + rc^*)$. h, k and l are integral numbers; ξ and η may take non-integral values.

	$p(a^*)$	$q(b^*)$	$r(c^*)$	
I	h	k	l	sharp spots
II	$h \pm \frac{1}{4}$	$k \pm \frac{1}{4}$	$l \neq 0$	diffuse maxima
	$h \pm \frac{1}{2}$	$k \pm \frac{1}{4}$	$l \neq 0$	
III	$h \pm \frac{1}{2}$	η	$l \neq 0$	streaks
	ξ	$k \pm \frac{1}{2}$	$l \neq 0$	

Tables for X-ray Crystallography (1968). The atomic coordinates are listed in Table 3.*

The average structure viewed along *c* is shown in Fig. 2(*a*). Each TCNQ molecule lies at ($\frac{1}{2}$,0,0) (hereafter named site I) or (0,$\frac{1}{2}$,0) (site II). The angle between the molecular plane and (001) is 30·2 or −30·2° [Fig. 2(*b*)]. In the average structure, these two orientations appear with equal probability. However, the intermolecular contact [Fig. 2(*b*)] suggests that in the actual structure, TCNQ anions are regularly stacked face-to-face along *c* to form a monadic column; this was confirmed later by analysis of the diffuse scattering. The mode of intermolecular overlap is of the 'ring–external-bond type' as illustrated in Fig. 3. A similar type of overlapping is found in all the crystals containing monadic columns of TCNQ at room temperature [NMP–TCNQ (Fritchie, 1966), TTF–TCNQ (Kistenmacher, Phillips & Cowan, 1974), TMTTF–TCNQ (Kistenmacher, Phillips, Cowan, Ferraris & Bloch, 1976), TTT–TCNQ (Shibaeva & Rosenberg, 1976), Rb–TCNQ–II (Shirotani & Kobayashi, 1973), Q–$TCNQ_2$ (Kobayashi, Marumo & Saito, 1971), ARD–$TCNQ_2$ (Kobayashi, 1974) and Rb–TCNQ–III (van Bodegom, de Boer & Vos, 1977), where NMP is *N*-methylphenazinium, TTF is tetrathiafulvalenium, TMTTF is tetramethyltetrathiafulvalenium, TTT is tetrathiotetracene, Q is quinolinium and ARD is acridinium]. The interplanar distance between neighbouring TCNQ anions reflects the magnitude of the charge-transfer interaction. The distance for NH_4–TCNQ–II (3·31 ± 0·02 Å) is comparable to that for Rb–TCNQ–III (3·32 Å) but is longer than those for highly conductive salts such as NMP–TCNQ (3·26), TTF–TCNQ (3·17), Q–$TCNQ_2$ (3·22) and ARD–$TCNQ_2$ (3·25 Å). The least-squares plane for TCNQ is $-0{\cdot}3537X + 0{\cdot}3511(Y - b/2) + 0{\cdot}8669Z = 0$, where *X*, *Y* and *Z* are coordinates (in Å) referred to the crystal axes *a*, *b* and *c* respectively. The deviations of the atoms are: C(1), −0·033; C(2), −0·015; C(3), 0·047; C(4), 0·052; N(2), −0·058 Å. Some intermolecular contacts are listed in Table 4. The distances between the nitrogen atoms of NH_4^+ and TCNQ suggest the existence of hydrogen bonds of the

* Lists of structure factors and anisotropic thermal parameters have been deposited with the British Library Lending Division as Supplementary Publication No. SUP 33564 (3 pp.). Copies may be obtained through The Executive Secretary, International Union of Crystallography, 5 Abbey Square, Chester CH1 2HU, England.

Table 3. *Fractional atomic coordinates with estimated standard deviations in parentheses*

	x (×10⁴)	*y* (×10⁴)	*z* (×10³)
C(1)	1016 (5)	5358 (5)	78 (2)
C(2)	686 (14)	4314 (14)	178 (3)
C(3)	1404 (13)	3596 (13)	388 (3)
C(4)	2451 (6)	3930 (6)	485 (4)
N(1)	0	0	0
N(2)	3256 (5)	4169 (5)	528 (7)
H	1877 (40)	5722 (39)	110 (24)

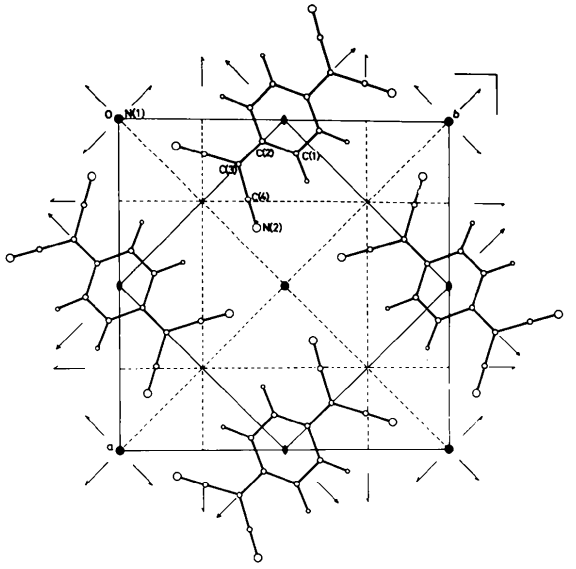

(*a*)

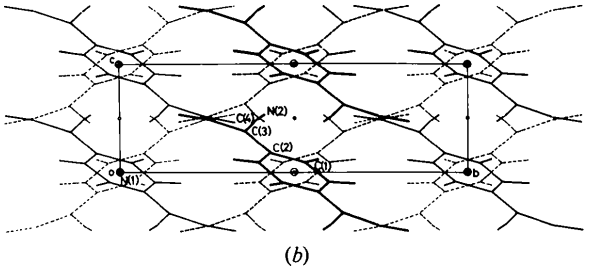

(*b*)

Fig. 2. The average structure. (*a*) Projection along *c*. (*b*) Projection along *a*: 'up' and 'down' TCNQ molecules are drawn with solid lines and broken lines respectively.

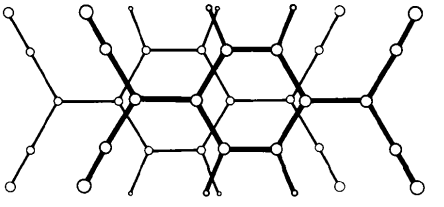

Fig. 3. Nearest-neighbour overlap of TCNQ.

Table 4. *Interatomic distances* (Å)

Symmetry code: (i) *x*,*y*,*z*; (ii) $\frac{1}{2}-y, \frac{1}{2}-x, z$; (iii) $\frac{1}{2}-y, \frac{1}{2}-x, z-1$; (iv) $x, y, z+1$; (v) $y, 1-x, z$; (vi) $y, 1-x, 1-z$.

$N(1^i)\cdots N(2^{ii})$	3·15 (3)	$C(4^i)\cdots C(1^{iv})$	3·40 (2)
$N(1^i)\cdots N(2^{iii})$	3·02 (3)	$N(2^i)\cdots N(2^v)$	3·42 (5)
$C(2^i)\cdots C(3^{iii})$	3·28 (2)	$N(2^i)\cdots N(2^{vi})$	3·43 (5)

type N—H···N. The difference synthesis gave broad peaks around the nitrogen atom of NH_4^+ indicating the positions of the hydrogen atoms. The atomic parameters, however, could not be refined successfully.

The bond lengths and angles of TCNQ are shown in Fig. 4.

Interpretation of the diffuse scattering

The two possible orientations of the TCNQ molecule shown in Fig. 2(*b*) are conveniently named 'up' and 'down' (↑,↓). Let us introduce the terms n_j and l_j:

when site I of the jth lattice is occupied by $\begin{cases} TCNQ_1^{\uparrow}, n_j = 1 \\ TCNQ_1^{\downarrow}, n_j = 0 \end{cases}$

and

when site II of the jth lattice is occupied by $\begin{cases} TCNQ_2^{\uparrow}, l_j = 1 \\ TCNQ_2^{\downarrow}, l_j = 0, \end{cases}$

where $TCNQ_1^{\uparrow}$ ($TCNQ_2^{\uparrow}$) stands for the 'up' TCNQ molecule located at site I (site II).

Disregarding the contribution from the hydrogen atoms of NH_4^+, the structure factor is given by

$$F(k) = \sum_j [f_N + f_{N'} + f_I^{\uparrow} n_j + f_I^{\downarrow}(1 - n_j) + f_{II\,j}^{\uparrow} + f_{II}^{\downarrow}(1 - l_j)] \exp(ikR_j),$$
$$k = 2\pi(\xi a^* + \eta b^* + \zeta c^*),$$

where the contributions from the nitrogen atoms of NH_4^+ located at (0,0,0) and $(\frac{1}{2},\frac{1}{2},0)$ are denoted as f_N and $f_{N'}$, respectively and $f_m^{\uparrow(\text{or}\downarrow)}$ (m = I or II) is the contribution of $TCNQ^{\uparrow(\text{or}\downarrow)}$ at the site m. The corresponding intensity is given by $I(k) = \langle |F(k)|^2 \rangle = I_B + I_D$ where

$$I_B = |\sum_j [f_N + f_{N'} + \langle n \rangle f_I^{\uparrow} + (1 - \langle n \rangle) f_I^{\downarrow} + \langle l \rangle f_{II}^{\uparrow} + (1 - \langle l \rangle) f_{II}^{\downarrow}] \exp(ikR_j)|^2$$

and

$$I_D = \sum_{jj'} \{\chi^{11}(j,j') |f_I^{\uparrow} - f_I^{\downarrow}|^2 + \chi^{22}(j,j') |f_{II}^{\uparrow} - f_{II}^{\downarrow}|^2 + \chi^{12}(j,j')[(f_I^{\uparrow} - f_I^{\downarrow}) * (f_{II}^{\uparrow} - f_{II}^{\downarrow}) + (f_{II}^{\uparrow} - f_{II}^{\downarrow}) * (f_I^{\uparrow} - f_I^{\downarrow})]\} \exp(ikR_{jj'})$$

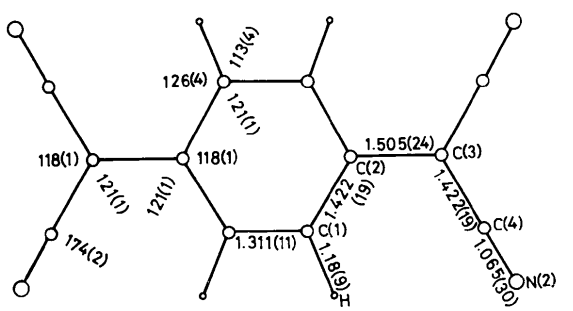

Fig. 4. Bond lengths (Å) and angles (°) with their standard deviations in parentheses.

where $R_{jj'}$ ($= R_j - R_{j'}$) $= m_1 a + m_2 b + m_3 c$, $\langle\rangle$ indicates the statistical average and $\chi^{11}(j,j')$, $\chi^{22}(j,j')$ and $\chi^{12}(j,j')$ are the following functions expressed as

$$\chi^{11}(j,j') = \langle (n_j - \langle n \rangle)(n_{j'} - \langle n \rangle) \rangle$$
$$\chi^{22}(j,j') = \langle (l_j - \langle l \rangle)(l_{j'} - \langle l \rangle) \rangle$$
$$\chi^{12}(j,j') = \langle (n_j - \langle n \rangle)(l_{j'} - \langle l \rangle) \rangle.$$

I_B gives the intensity of a sharp spot. As described in the preceding section, both $\langle n \rangle$ and $\langle l \rangle$ are $\frac{1}{2}$. The second term I_D gives the intensities of the diffuse scattering. Since diffuse streaks along a^* and b^* are due to the stacking disorder along a and b respectively, the diffraction patterns shown in Fig. 1 indicate that the domains containing the stacking disorder along a and b co-exist in the crystal.

A domain which gives the streaks along b^* will now be considered. The intensity distribution of the diffuse scattering was explained by the following considerations, listed in (i)–(v):

(i) Since there are two sites and two possible orientations of the TCNQ molecules, four types of superstructures can be deduced, of which the lattice constants are $a' = 2a$, $b' = 4a$ and $c' = c$, and these are shown in Fig. 5(*a*), (*b*), (*c*) and (*d*). The structures are related to each other by twinning axes parallel to c or twinning planes perpendicular to b. One fixed orientation of the TCNQ molecule is repeated along c. The two orientations of the TCNQ molecules appear alternately along a and they alternate for every two molecules along b.

(ii) The procedure for the calculation of χ^{11} and χ^{22} is as follows:

(1) When both n_j and $n_{j'} = 1$ or 0, $(n_j - \langle n \rangle)(n_{j'} - \langle n \rangle) = \frac{1}{4}$, where $\langle n \rangle$ was assumed to be $\frac{1}{2}$. Similarly for two TCNQ molecules having the opposite orientations, $(n_j - \langle n \rangle)(n_{j'} - \langle n \rangle) = -\frac{1}{4}$. The same scheme is valid for $(l_j - \langle l \rangle)(l_{j'} - \langle l \rangle)$.

(2) If $R_{jj'} = m_1 a + m_3 c$, $\chi^{11}(j,j') = \chi^{22}(j,j') = (-1)^{m_1}/4$.

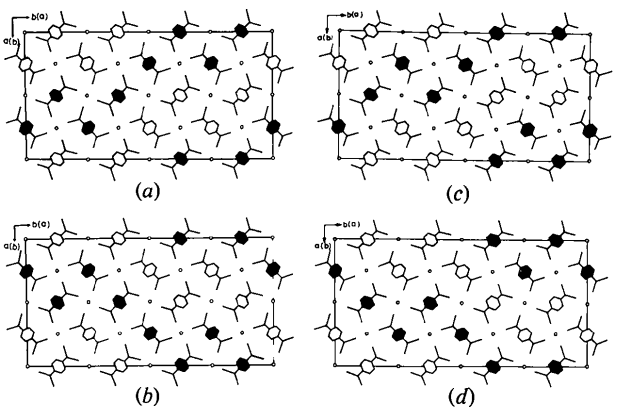

Fig. 5. The structural models of the domains. The open and closed hexagons indicate 'up' and 'down' TCNQ molecules respectively.

(3) If the orientations of two $TCNQ_1$ molecules (or $TCNQ_2$ molecules) located at R_j and $R_j + b$ are identical (*e.g.* ↑↑), the mode of the molecular orientation along b is represented schematically by

$$\ldots\uparrow(-4).\uparrow(-3).\downarrow(-2).\downarrow(-1).\uparrow(0).\uparrow(1).\downarrow(2).\downarrow(3).\uparrow(4)\ldots$$

where the symbol $\uparrow(m_2)$ represents 'up' $TCNQ_1$ ($TCNQ_2$) located at $R_j + m_2 b$. When the orientation of the two TCNQ molecules is different (*e.g.* ↑↓) the mode of the molecular arrangement is represented by

$$\ldots\uparrow(-4).\downarrow(-3).\downarrow(-2).\uparrow(-1).\uparrow(0).\downarrow(1).\downarrow(2).\uparrow(3).\uparrow(4)\ldots$$

(4) After calculation, we have

$$\sum_j \chi^{11}(j,j') = \sum_j \chi^{11}(j,m_1,m_2,m_3)$$
$$= N(-1)^{m_1}/4 \times \begin{cases} 1 \ldots m_2 = \ldots, 0, 4, 8, 12, \ldots \\ 0 \ldots m_2 = \ldots, 1, 3, 5, 7, \ldots \\ -1 \ldots m_2 = \ldots, 2, 6, 10, 14, \ldots \end{cases}$$
$$= N(-1)^{m_1} \cos(\pi m_2/2)/4$$

where $R_{jj'} = m_1 a + m_2 b + m_3 c$ and N is the number of the unit cells. The same equation holds for $\sum_j \chi^{22}(j,m_1,m_2,m_3)$.

(iii) The distribution of diffuse streaks in the reciprocal space indicates that the stacking disorder occurs along the longest axis of the superlattices. In a crystal containing stacking disorder along b, the following equation must be satisfied:

$$\lim_{|m_2| \to \infty} \chi^{11}(j,m_1,m_2,m_3) = 0.$$

In this paper, the magnitude of $\chi^{11}(j,m_1,m_2,m_3)$ was assumed to decrease exponentially with increase in $|m_2|$. The following equation is then derived

$$\sum_j \chi^{11}(j,m_1,m_2,m_3) = \sum_j \chi^{22}(j,m_1,m_2,m_3)$$
$$= N(-1)^{m_1} \exp(-\alpha|m_2|) \cos(\pi m_2/2)/4$$

where α is a damping parameter.

(iv) A similar equation can be derived for χ^{12}. However, there is no need to derive the equation if a crystal contains an equal amount of the domains shown in Fig. 5(*a*) and (*b*) and/or (*c*) and (*d*). This can be seen from the following consideration. When the mode of the arrangement of $TCNQ_2$ along b is

$$\ldots\uparrow(0).\uparrow(1).\downarrow(2).\downarrow(3).\uparrow(4).\uparrow(5)\ldots,$$

the modes of the arrangements of $TCNQ_1$ are

$$\ldots\uparrow(0).\uparrow(1).\downarrow(2).\downarrow(3).\uparrow(4).\uparrow(5)\ldots$$

and

$$\ldots\downarrow(0).\downarrow(1).\uparrow(2).\uparrow(3).\downarrow(4).\downarrow(5)\ldots$$

for the domains shown in Fig. 5(*a*) and (*b*) respectively; that is, the orientation of $TCNQ_1$ is inverted for these two structures. Consequently, the values of χ^{12} for these two domains are equal in magnitude but opposite in sign and they do not contribute to I_D.

(v) I_D can thus be written as

$$I_D = N/4 \sum_{m_1 m_2 m_3} (|f_I^{\uparrow} - f_I^{\downarrow}|^2 + |f_{II}^{\uparrow} - f_{II}^{\downarrow}|^2)$$
$$\times (-1)^{m_1} \exp(-|m_2|\alpha)$$
$$\times \cos(\pi m_2/2) \cos[2\pi(\xi m_1 + \eta m_2 + \zeta m_3)]$$
$$= N_2 N_1^2 N_3^2 (|f_I^{\uparrow} - f_I^{\downarrow}|^2 + |f_{II}^{\uparrow} - f_{II}^{\downarrow}|^2)$$
$$\times \delta(\zeta - l)\, \delta(\xi - h \pm \tfrac{1}{2})$$
$$\times (1 - A^2)/\{1 + A^2 - 2A \cos[2\pi(\eta \pm \tfrac{1}{4})]\}$$

where $A = \exp(-\alpha)$.

The intensities were calculated for various values of A (= 0·1, 0·2, 0·3,..., 0·9) and were compared with the observed intensities. The observed intensities of the streaks were estimated visually with a standard film strip. Then I_D^{obs} was given by

$$I_D^{obs}(h \pm \tfrac{1}{2}, \eta, l) \propto I(h \pm \tfrac{1}{2}, \eta, l)\, \mathrm{Lp}(1 + s)(\delta S/\delta X)_{\parallel} \times (\delta S/\delta X)_{\perp}$$

where Lp^{-1} is the Lorentz and polarization correction, s is the shape factor and $(\delta S/\delta X)_{\parallel}$ and $(\delta S/\delta X)_{\perp}$ are the geometrical factors (Takaki, Kato & Sakurai, 1975) for the contraction or expansion of the streaks. The geometrical factors were calculated by use of the equation $2\theta' = \omega \pm \cos^{-1}(\cos\omega + \lambda d^*/\cos\nu)$, where $\parallel$ and $\perp$ indicate the directions parallel (length) and perpendicular (width) to the streaks in the reciprocal space, respectively. A segment on a Weissenberg film δS and the corresponding segment in the reciprocal space δX (Takaki, Kato & Sakurai, 1975) are given by

$$\delta S(\omega) = \sqrt{\{(\delta\omega/2)^2 + [\theta'(\omega) - \theta'(\omega + \delta\omega)]^2\}}$$
$$\delta X(\omega) = \sqrt{[(2\cos\nu(\lambda)^2 \sin^2\theta'(\omega + \delta\omega) - d^{*2}]} - \sqrt{[(2\cos\nu/\lambda)^2 \sin^2\theta'(\omega) - d^{*2}]}.$$

where (ω,θ') is a coordinate on the film, representing a position along the Weissenberg chart and ν is an equi-inclination angle. When A = 0·7, the calculated intensities appear to be in fairly good agreement with the observed intensities. Fig. 6 shows an example of the comparison of the observed and calculated intensities along the streaks. If $k = 2\pi(\xi a^* + \eta b^*)$, the molecular structure factor of the 'up' TCNQ molecule is equal to that of the 'down' molecule. For this reason diffuse scattering does not appear on the equator (Fig. 1).

It is worthwhile to point out that each structure shown in Fig. 5(*a*)–(*d*) can be regarded as a kind of 'anti-phase domain structure' where the length of the 'out-of-step vector' is a (= $a'/2$) and M is 2 [Ma (= $b'/2$) is the length of the anti-phase domain]. Probably NH_4–TCNQ–II is the first documented example of the anti-phase domain structure of a molecular complex.

Phase transition of NH_4–TCNQ

The temperature change of the patterns in the oscillation photographs for the NH_4–TCNQ–I crystal around the needle axis was examined. At low temperature (t <28·5 °C), strong and weak layer lines appeared alternately. The weak layer lines disappeared at t >28·5 °C. The lattice constant of the high-temperature modification (c = 3·611 Å at 38 °C) indicates the existence of a monadic column of TCNQ molecules. The doubling of the lattice constant at low temperatures (c = 7·189 Å at 20 °C) shows the occurrence of a monomer–dimer (M–D) transition.

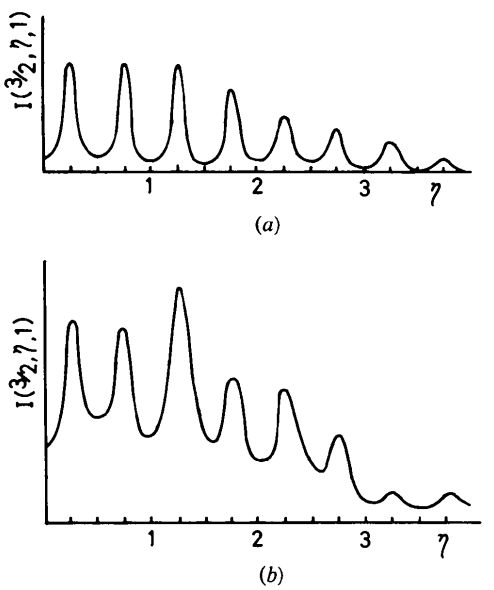

Fig. 6. The intensities of a streak. (*a*) Calculated (A = 0·7). (*b*) Observed.

The X-ray transition temperature, 28·5 ± 5 °C, agrees with the magnetic transition temperature [26 °C (Vegter & Kommandeur, 1975)]. Thus, the NH_4–TCNQ used was NH_4–TCNQ–I. A similar examination was made for the new form of NH_4–TCNQ, *i.e.* NH_4–TCNQ–II. However, no X-ray evidence for a M–D transition could be obtained in the temperature range from −50 to 50 °C. Therefore, the d.c. resistivity was measured along c by use of the four-probe technique in order to obtain evidence of a M–D transition (120 < T < 304 K). Four 25 μm gold wires were bonded to the crystal with du Pont 4817 conducting paint. The approximate dimensions of the two specimens used were 0·35 × 0·45 × 3·0 mm and 0·55 × 0·53 × 3·0 mm. The room-temperature resistivities, R_o of the two samples were 8·8 × 10^2 and 2·9 × 10^2 Ωcm. A change in the slope of the log R/R_o *vs* $1/T$ curve suggested a M–D transition (Fig. 7). A similar change has been reported for powdered samples of TTF–TCNQ and this was attributed to the occurrence of a metal–insulator transition (Viswanathan & Johnston, 1975). Anomalies in the log R *vs* $1/T$ curves have also been observed at the M–D transition temperatures for Na–TCNQ, K–TCNQ and Rb–TCNQ–I (Sakai, Shirotani & Minomura, 1972).

Polymorphism of a simple salt of TCNQ has been found for Rb–TCNQ (Hoekstra, Spoelder & Vos, 1972; Shirotani & Kobayashi, 1973; van Bodegom, de Boer & Vos, 1977). The physical properties of Rb–TCNQ are compared with those of NH_4–TCNQ in Table 5. Since the column structure of NH_4–TCNQ–II resembles that of Rb–TCNQ–II, it is possible that the colours and the electrical conductivities of these salts may bear a close similarity.

The information about the crystal structures and the magnetic susceptibilities so far obtained suggests that

Table 5. *Physical properties of* Rb–TCNQ *and* NH_4–TCNQ

	Rb–TCNQ–I	Rb–TCNQ–II	Rb–TCNQ–III	NH_4–TCNQ–I	NH_4–TCNQ–II
Colour	reddish-purple	dark purple	–	purple	bluish-purple
Electrical resistivity (RT) (Ωcm)	3 × 10^5	1 × 10^2	–	–	5 × 10^2
Activation energy (RT) (eV)	0·44–0·53	0·16–0·22	–	–	0·21
Transition temperature (K)*	376_m 373_x	220_m 230_x	–	299_m 301_x	215_e
Periodicity of TCNQ column at RT	diad	monad	monad	diad	monad
Mode of overlap of TCNQ†	*A*	*B*	*B*	–	*B*
Intermolecular distance (RT) (Å)	3·48‡ 3·17	3·43	3·33	–	3·31

* m, x and e indicate the transition temperatures determined by magnetic susceptibility, X-ray diffraction and electrical conductivity, respectively.

† *A*: ring–ring type. *B*: ring–external-bond type.

‡ Two independent intermolecular distances which appear alternately in a diadic column of TCNQ.

every member of the family of alkali-metal–TCNQ, except Li–TCNQ, undergoes a *M–D* transition; the transition temperature of Li–TCNQ appears to be too high for the transition to be observed [$T_c > 450$ K (Kommandeur, 1975)]. Fig. 8 shows the relation between T_c and d, where T_c is the transition temperature and d is the interplanar distance of $TCNQ^-$ anions in a monadic column of the high-temperature structure. A *M–D* transition appears in 'the phase diagram' for $d > 3{\cdot}3$ Å. Also T_c decreases with d. In Fig. 9, T_c is plotted against δd ($= d_1 - d_2$, where d_1 and d_2 are the two interplanar distances which appear alternately in a dimeric column of the low-temperature structure): δd = 0·346, 0·314 Å (K–TCNQ); 0·282, 0·280 Å (Na–TCNQ); 0·325 Å (Rb–TCNQ–I) (Konno & Saito, 1974; Konno, Ishii & Saito, 1977; Hoekstra, Spoelder & Vos, 1972). There is a linear relationship between T_c and δd: $\delta d/T_c = 8{\cdot}4 \times 10^{-4}$ (K–TCNQ), $8{\cdot}1 \times 10^{-4}$ (Na–TCNQ) and $8{\cdot}6 \times 10^{-4}$ (Rb–TCNQ–I).

Recent studies have shown that a regular antiferromagnetic chain becomes unstable at low temperatures ($T < T_c$) and transforms to a dimeric chain (spin–Peierls transition) (Pytte, 1974; Bray *et al.*, 1975). The column structure and the comparatively large intermolecular distance suggest that the *M–D* transition of alkali-metal–TCNQ can be regarded as a spin–Peierls transition.

The temperature dependence of the magnetic susceptibility $\chi(T)$ of a dimeric chain ($T < T_c$) is given by: $\chi(T) = C\exp(-\Delta/T)/T$ (Bulaevskii, 1969). Based on the magnetic data reported by Kommandeur (1975), Δ/T_c can be estimated roughly as: 7·0 (Na–TCNQ),

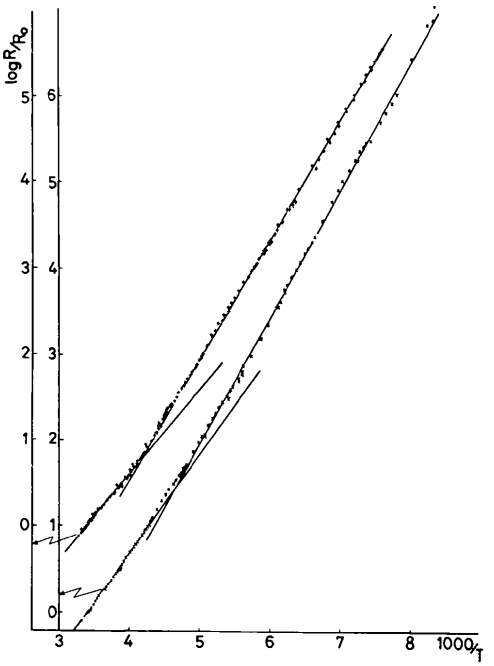

Fig. 7. Activation plot of normalized resistivity of NH_4–TCNQ–II.

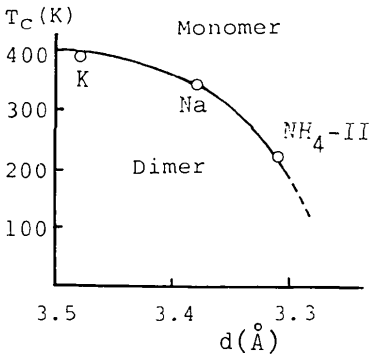

Fig. 8. The relationship between transition temperature (T_c) and the interplanar distance of TCNQ (d).

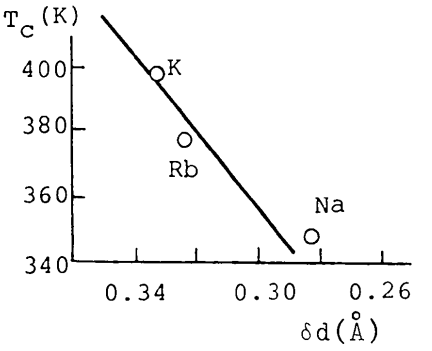

Fig. 9. The relationship between transition temperature (T_c) and the difference between two interplanar distances which appear alternately in a dimeric column of TCNQ ($\delta d = d_1 - d_2$). Solid line represents the relationship, $\delta d/T_c = 8{\cdot}4 \times 10^{-4}$. δd of K–TCNQ and Na–TCNQ are the mean values.

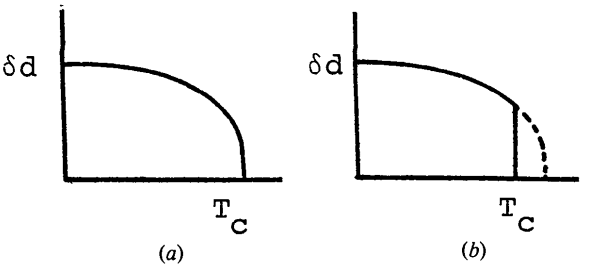

Fig. 10. Schematic representation of the relationship between the variation of δd and T_c. (*a*) Second-order phase transition. (*b*) First-order phase transition.

9·0 (K–TCNQ), 8·6 (Rb–TCNQ–I) and 8·3 (NH_4–TCNQ–I). Since the phase transitions of these salts except Na–TCNQ are first-order ones, T_c will be smaller than the transition temperature which would be obtained if the transitions were second-order (Fig. 10). Therefore, Δ/T_c for K–TCNQ, Rb–TCNQ–I and NH_4–TCNQ–I may have been overestimated. Consequently, Δ/T_c appears to be constant (~7·0) in these systems. The constancy of Δ/T_c and the linear relationship between δd and T_c (Fig. 9) strongly suggest a spin–Peierls mechanism for the transition.

A donor–acceptor complex, TTF–$CuS_4C_4(CF_3)_4$ has been reported to be the first example of a spin–Peierls system, where good agreement was obtained between experiment and the mean-field theory of the spin–Peierls transition (Bray *et al.*, 1975). Using the magnetic data of TTF–$CuS_4C_4(CF_3)_4$ reported by Bray *et al.* (1975), we find the ratio, Δ/T_c to be 3·5, which is about one half of the ratio for alkali-metal–TCNQ. This difference can be explained if the fluctuation theory of the Peierls transition (Lee, Rice & Anderson, 1973) can be applied to the spin–Peierls transition: (1) Owing to the fluctuation neglected in the mean-field theory, the linear system does not have an effective gap near T_p (the transition temperature deduced in the mean-field approximation) and the real transition temperature T_c is lowered; (2) T_c varies with the magnitude of the interchain coupling (Dieterich, 1975). The fluctuation effect has been observed in the Peierls transition of one-dimensional metal systems such as $K_2Pt(CN)_4Br_{0.3}.3H_2O$, TTF–TCNQ and $TTF(SCN)_x$ (Bulaevskii, 1975; Etemad, 1976; Somoano, Gupta, Hadek, Novotny, Jones, Datta, Deck & Herman, 1977). The ratios Δ/T_c are about three times larger than the mean-field value (T_c is the Peierls transition temperature and 2Δ is the band gap).

The column structure of alkali-metal–TCNQ compounds resembles that of TTF–TCNQ. The latter system undergoes a Peierls transition accompanied by fluctuation unlike that of 'the alternate column' of the TTF–$CuS_4C_4(CF_3)_4$ system where the mean-field theory is valid. Considering the parallelism between the theories of the Peierls and spin–Peierls transitions, it appears that the mean-field theory is insufficient to explain the *M–D* transition. Thus, it may be said that the *M–D* transition of *M*-TCNQ can be regarded as a spin–Peierls transition which accompanies the fluctuation.

References

André, J. J., Bieber, A. & Gautier, F. (1976). *Ann. Phys. (Paris)*, **1**, 145–256.

Bodegom, B. van, de Boer, J. L. & Vos, A. (1977). *Acta Cryst.* B**33**, 602–604.

Bray, J. W., Hart, H. R. Jr, Interrante, L. V., Jacobs, I. S., Kasper, J. S., Watkins, G. D., Wee, S. H. & Bonner, J. C. (1975). *Phys. Rev. Lett.* **35**, 744–747.

Bulaevskii, L. N. (1969). *Sov. Phys. Solid State*, **11**, 921–924.

Bulaevskii, L. N. (1975). *Soviet Phys. Usp.* **18**, 131–150.

Dieterich, W. (1975). *One-Dimensional Conductor*, edited by J. Ehlers, K. Hepp & H. A. Weidenmuller. Berlin: Springer.

Etemad, S. (1976). *Phys. Rev. B*, **13**, 2254–2261.

Fritchie, C. J. (1966). *Acta Cryst.* **20**, 892–898.

Hoekstra, A., Spoelder, T. & Vos, A. (1972). *Acta Cryst.* B**28**, 14–25.

International Tables for X-ray Crystallography (1968). Vol. III, 2nd ed. Birmingham: Kynoch Press.

Keller, H. J. (1977). Editor, *Chemistry and Physics of One-Dimensional Metals*. New York: Plenum.

Kistenmacher, T. J., Phillips, T. E. & Cowan, D. O. (1974). *Acta Cryst.* B**30**, 763–768.

Kistenmacher, T. J., Phillips, T. E., Cowan, D. O., Ferraris, J. P. & Bloch, A. N. (1976). *Acta Cryst.* B**32**, 539–547.

Kobayashi, H. (1974). *Bull. Chem. Soc. Jpn*, **47**, 1346–1352.

Kobayashi, H., Marumo, F. & Saito, Y. (1971). *Acta Cryst.* B**27**, 373–378.

Kommandeur, J. (1975). *Low-Dimensional Cooperative Phenomena*, edited by H. J. Keller. NATO ASI, Series B, Vol. 7. New York: Plenum.

Konno, M., Ishii, T. & Saito, Y. (1977). *Acta Cryst.* B**33**, 763–770.

Konno, M. & Saito, Y. (1974). *Acta Cryst.* B**30**, 1294–1299.

Konno, M. & Saito, Y. (1975). *Acta Cryst.* B**31**, 2007–2012.

Lee, P. A., Rice, T. M. & Anderson, P. W. (1973). *Phys. Rev. Lett.* **31**, 462–465.

Pytte, E. (1974). *Phys. Rev. B*, **10**, 4637–4642.

Sakai, N., Shirotani, I. & Minomura, S. (1972). *Bull. Chem. Soc. Jpn*, **45**, 3314–3328.

Shibaeva, R. P. & Rosenberg, L. P. (1976). *Sov. Phys. Crystallogr.* **20**, 581–583.

Shirotani, I. & Kobayashi, H. (1973). *Bull. Chem. Soc. Jpn*, **46**, 2595–2596.

Somoano, R. B., Gupta, A., Hadek, V., Novotny, M., Jones, M., Datta, T., Deck, R. & Herman, A. M. (1977). *Phys. Rev. B*, **15**, 595–601.

Takaki, Y., Kato, Y. & Sakurai, K. (1975). *Acta Cryst.* B**31**, 2753–2758.

Vegter, J. G. & Kommandeur, J. (1975). *Mol. Cryst. Liq. Cryst.* **30**, 11–39.

Vegter, J. G., Kuindersma, P. I. & Kommandeur, J. (1971). *Conduction in Low-Mobility Materials*, edited by N. Klein, D. S. Tannhauser & M. Pollak, pp. 363–373. London: Taylor & Francis.

Viswanathan, R. & Johnston, D. C. (1975). *J. Phys. Chem. Solids*, **36**, 1093–1096.